chemosensors

Article

Ferrocene-Containing Gallic Acid-Derivative Modified Carbon-Nanotube Electrodes for the Fast Simultaneous and Selective Determination of Cytostatics from Aqueous Solutions

Sorina Motoc (m. Ilies) [1], Adelina Andelescu [1], Alexandru Visan [1], Anamaria Baciu [2], Elisabeta I. Szerb [1] and Florica Manea [2,*]

[1] "Coriolan Drăgulescu" Institute of Chemistry, Romanian Academy, 24 Mihai Viteazu Bvd., 300223 Timisoara, Romania; sorinailies@acad-icht.tm.edu.ro (S.M.); aandelescu@acad-icht.tm.edu.ro (A.A.); visan.alexandru@acad-icht.tm.edu.ro (A.V.); eszerb@acad-icht.tm.edu.ro (E.I.S.)
[2] Department of Applied Chemistry and Engineering of Inorganic Compounds and Environment, Politehnica University of Timisoara, Bvd. Vasile Parvan No. 6, 300223 Timisoara, Romania; anamaria.baciu@upt.ro
* Correspondence: florica.manea@upt.ro

Abstract: In this work, a ferrocene-containing gallic acid-derivative modified carbon-nanotube paste electrode (Gal-Fc-CNT), obtained through simple mechanical mixing, was studied for the fast simultaneous voltammetric determination of doxorubicin (DOX), capecitabine (CPB), and cyclophosphamide (CPP) as cytostatic indices based on their cumulative signals and the selective determination of DOX. The individual and simultaneous electrochemical behavior of DOX, CPB, and CPP, studied through cyclic voltammetry (CV) on the Gal-Fc-CNT paste electrode at various pHs and potential ranges, allowed for the development of a simple simultaneous determination method as a cytostatic index at a pH of 12 using square-wave voltammetry, which allowed for a better performance than reported electrodes for each individual cytostatic. A faster and selective detection of DOX, with a limit of detection of 75 ng·L^{-1}, was achieved using square-wave voltammetry at a pH of 3. The good results obtained for the real tap water assessment indicated the applicability of the Gal-Fc-CNT paste electrode for practical applications (water samples).

Keywords: ferrocene-modified carbon-nanotube paste electrode; square-wave voltammetry; cytostatic; selective/simultaneous voltammetric determination

Citation: Motoc, S.; Andelescu, A.; Visan, A.; Baciu, A.; Szerb, E.I.; Manea, F. Ferrocene-Containing Gallic Acid-Derivative Modified Carbon-Nanotube Electrodes for the Fast Simultaneous and Selective Determination of Cytostatics from Aqueous Solutions. *Chemosensors* **2024**, *12*, 15. https://doi.org/10.3390/chemosensors12010015

Academic Editor: Pedro Salazar

Received: 5 December 2023
Revised: 15 January 2024
Accepted: 17 January 2024
Published: 19 January 2024

Correction Statement: This article has been republished with a minor change. The change does not affect the scientific content of the article and further details are available within the backmatter of the website version of this article.

1. Introduction

Considering the role of pharmaceuticals in improving quality of life, their presence in the environment is increasing, thus representing a new class of emerging environmental contaminants [1–3] that necessitate growing attention related to their environmental impact and human health risk, because they are constantly released into aquatic environments [1] through wastewater treatment plants, human and animal excretion, and surface waters or soils [3].

The most studied pharmaceuticals are antibiotics, painkillers, and cardiovascular drugs due to their worldwide use [4]. Taking into account that the leading cause of death worldwide is cancer [5], the production and consumption of another class of pharmaceuticals—cytostatics—is increasing, and therefore, their presence in the environment will increase [2,6]. Besides their ability to kill tumor cells, cytostatics are not specific to cancerous cells, also affecting healthy cells [7]. Once entered in the blood stream, these compounds are excreted in their unmetabolized form or as metabolites; the resulting effluents from hospitals, homes, and pharmacies reach the sewage system, with a negative impact on the health of both humans and ecosystems [6,8].

Cyclophosphamide (CPP, 2-[Bis(2-chloroethylamino)]-tetrahydro-2H-1,3,2-oxazaphosphorine-2-oxide) is an antineoplastic drug that is still being used to treat multiple myeloma, malig-

nant lymphomas, leukemias, and carcinoma of the breast [9]. Another cytostatic drug, doxorubicin (DOX, (7S,9S)-7-[(2R,4S,5S,6S)-4-amino5-hydroxy-6-methyloxan-2-yl]oxy-6,9,11-trihydroxy-9-(2-hydroxyacetyl)-4-methoxy-8,10-dihydro-7H-tetracene-5,12-dione), which belongs to the class of anthracycline antibiotics, is used for treating solid tumors, leukemia, lymphomas, and breast cancer. Capecitabine (CPB, pentyl[1-(3,4-dihydroxy-5-methyltetrahydrofuran-2-yl)-5-fluoro-2-oxo-1H-pyrimidin-4-yl] carbamate) is an oral chemotherapeutic agent used in the treatment of breast, esophageal and larynx, gastrointestinal, and genitourinary tract cancers, and is commonly reported to be present in water [10].

Although the concentrations reported in surface water for cytostatics are usually below the concentration (or dose) that is effective in producing 50% of the maximal response (EC50) reported for a range of aquatic organisms [11], their toxicological properties combined with their poor biodegradability could have a negative impact on human and ecological health, even at very low concentrations. Therefore, it is important to assess the occurrence and fate of anticancer drugs in the environment, since their consumption has increased and is expected to further increase in following years [6].

The current employed methods for the detection of cytostatic pollutants in environmental samples rely mostly on chromatographic methods, such as liquid chromatography coupled with mass spectrometry (LC–MS) [12,13]. Although sensitive and reliable, they present several disadvantages, such as being time-consuming and expensive techniques that require sample pre-treatment.

A promising and cheaper alternative could be electroanalytical methods, which have high sensitivity and a rapid response [10], and also, due to their ease of use, accuracy, and reliability, are able to determine the levels of electroactive species in a solution. The detection of pollutants in water can be realized through the use of voltammetric or amperometric sensors, which can be developed in relation to the electrode's composition together with electrochemical techniques [14].

The most important role in electrochemical sensing performance is played by the working electrode material; carbon-based electrode materials are very common and useful in electroanalysis, but are not always appropriate for detection at trace-level concentrations due to electrode process kinetics and slow electron mobility [15].

This disadvantage should be overcome by modifying carbon-based compositions through different modification procedures, resulting in so-called chemically modified carbon-based electrodes. Drop casting is the easiest and fastest technique for modifying electrodes that are applied to checking the electrocatalytic activity of modifiers towards target analytes, yet without good stability, while paste mixing is also an easy and cheap method for integrating the modifier within the electrode composition, characterized by greater stability [16]. A large spectrum of modifiers, including nanostructured carbons, have been reported for the modification of carbon-based materials through drop casting [17,18] and paste mixing [19–22]. Also, carbon nanotubes (CNTs) are well-known as porous nanostructures characterized by a high surface area, high electrical conductivity, significant mechanical strength, and chemical stability [20,21] making them suitable as both a modifier [23] and substrate [20–22].

Ferrocene (Fc), widely employed as an internal standard in electrochemistry, has a sandwich structure with d–π interactions between Fe(II) and the cyclopentadienyl rings, leading to unique chemical properties, the most important being the ability to undergo reversible oxidation to ferrocenium ion (Fc^+) [24]. Other key features of this molecule are its chemical stability, low toxicity, and ease of functionalization on either one or both of the cyclopentadienyl rings, maintaining the electrochemical reversibility of the parent molecule [25], leading to research on Fc and its derivatives for the development of electrochemical sensors for the detection of environmental pollutants [24]. Recently, ferrocene-containing gallic acid derivatives (Gal-Fc) have been characterized by our team, and have been found to possess properties that render them suitable as a candidate in sensing applications [26].

Gallic acid, or 3,4,5-trihydroxybenzoic acid, is a common polyphenolic compound found in plants [27]. Gallic acid and its derivatives are mostly researched due to its various biological activities, such as antibacterial, antiviral, anti-inflammatory, antitumor activities, etc. [28]. The presence of carboxylic and hydroxylic functional groups within this type of molecule makes them potential candidates for electrochemical applications; e.g., propyl gallate was used as a modifier in a modified paste electrode for the detection of low concentrations of uranium [29], while epigallocatechin gallate was used in the development of electrochemical sensors for the simultaneous detection of redox-active biomolecules, such as dopamine, uric acid, and ascorbic acid [30].

Based on the above-presented considerations and our preliminary reported results [26], the aim of this study is to modify carbon nanotubes (CNTs) with ferrocene-containing gallic acid derivatives (Gal-Fc) through paste mixing in paraffin oil to develop sensitive simultaneous and selective methods for the electrochemical determination of cytostatics, i.e., doxorubicin (DOX), capecitabine (CPB), and cyclophosphamide (CPP). Considering the electrocatalytic activity of Gal-Fc-CNT paste electrodes, differential-pulse and square-wave voltammetry are exploited to develop the simultaneous and selective determination of cytostatics in water samples. Several electrode compositions have been reported for the electrochemical determination of DOX [31–38], as well as a few for CPB through reduction processes [39,40] and for the electrochemical determination of CPP through anodic oxidation [41,42]. To the best of our knowledge, no simultaneous and/or selective voltammetric determinations of cytostatics on modified carbon-based electrodes have been reported.

2. Materials and Methods

The experimental details of the ferrocene-containing gallic acid-derivative synthesis are described in the Supplementary Materials—Scheme S1. The Gal-Fc compound, with the chemical structure presented in Figure 1, was obtained in a multi-step procedure according to our previously published work [26], and the synthetic route is presented in Supplementary Materials—Scheme S1. Briefly, compound I was obtained through the electrophilic aromatic substitution of the ferrocene ring with the acyl chloride of 11-bromoundecanoic acid, employing a Friedel–Crafts reaction [43], while the intermediate compound **2** was obtained by modifying the molar ratio between the gallic acid, the base (K_2CO_3), and the corresponding alkyl bromide to favor the formation of the desired compound (see Supplementary Materials). Gal-Fc was obtained after a Williamson etherification reaction between intermediate compound I and compound II, followed by the ester hydrolysis in basic media (Supplementary Materials—Scheme S1).

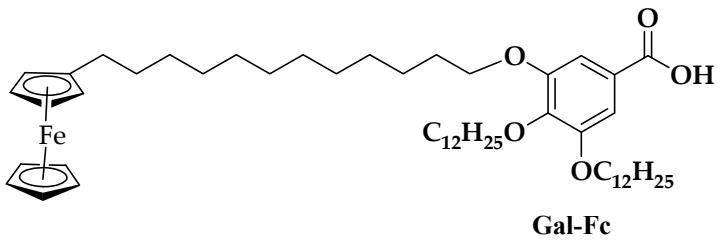

Gal-Fc

Figure 1. Proposed chemical structure of compound Gal-Fc.

Ferrocene, anhydrous aluminum chloride ($AlCl_3$), sodium borohydride ($NaBH_4$), dichloromethane (DCM), and tetrahydrofuran (THF) were purchased from Sigma Aldrich, Darmstadt, Germany, and were used as received. The solvents used for the column chromatography were technical-grade and were purchased from Carlo Erba, Emmendingen, Germany. Multiwall carbon nanotubes (CNTs), synthesized via catalytic carbon vapor deposition (CCVD), were purchased from Nanocyl^{TM}, Sambreville, Belgium. Standard stock solutions of 1 g·L^{-1} of doxorubicin (DOX), capecitabine (CPB), and cyclophosphamide (CPP) were prepared daily from analytical-grade Sigma Aldrich reagents using double-

distilled water. The supporting electrolyte for the characterization and application of the electrode material in the determination process was a 0.1 M NaOH solution, which was freshly prepared from NaOH of analytical purity (Merck, Darmstadt, Germany) with double-distilled water. Also, 0.1 M Na_2SO_4 was used as the supporting electrolyte, adjusted to pH values of 3 and 5 using 1 M H_2SO_4 of analytical purity (Merck).

Infrared spectra were recorded on a Cary 630 FT-IR spectrophotometer (Penang, Malaysia) in the range of 4000–400 cm^{-1} as KBr pellets.

The ^{1}H-NMR were recorded in $CDCl_3$ using a Bruker FOURIER 300 MHz (Karlsruhe, Germany).

A Flash 2000 microanalyzer from ThermoFisher Scientific (Dartford, UK) was used for CHN elemental analysis.

The working paste electrode was obtained through the simple mechanical mixing of a certain amount of carbon nanotubes (CNTs) with the ferrocene-containing gallic acid derivative (Gal-Fc) and paraffin oil to assure the weight ratio of Gal-Fc/CNT/oil = 1:1:2.5 for the Gal-Fc-CNT paste electrode.

The voltammetric techniques, i.e., cyclic voltammetry (CV), differential-pulsed voltammetry (DPV), and square-wave voltammetry (SWV), were employed at ambient room temperature (~20 °C) using an Autolab potentiostat/galvanostat PGSTAT 302N (EcoChemie, Utrecht, the Netherlands), controlled using the 4.9 GPES software (4.9 version). The classical three-electrode cell, consisting of the working Gal-Fc-CNT paste electrode, a saturated calomel reference electrode (SCE), and a platinum counter electrode (Pt), was used.

The limit of detection (LOD) and the limit of the quantification (LOQ) were determined with the equations of LOD = 3 SD/m and LQ = 10 SD/m, where SD is the standard deviation of three blanks and m is the slope of the analytical plots [19]. The reproducibility of the electrodes using the above-mentioned technique was evaluated based on the relative standard deviation (RSD) for three replicate measurements of DOX, CPB, and CPP concentrations.

3. Results

The intermediates and the targeted compound Gal-Fc were characterized via FT-IR (Figure 2) and ^{1}H-NMR spectroscopies (Figure 3).

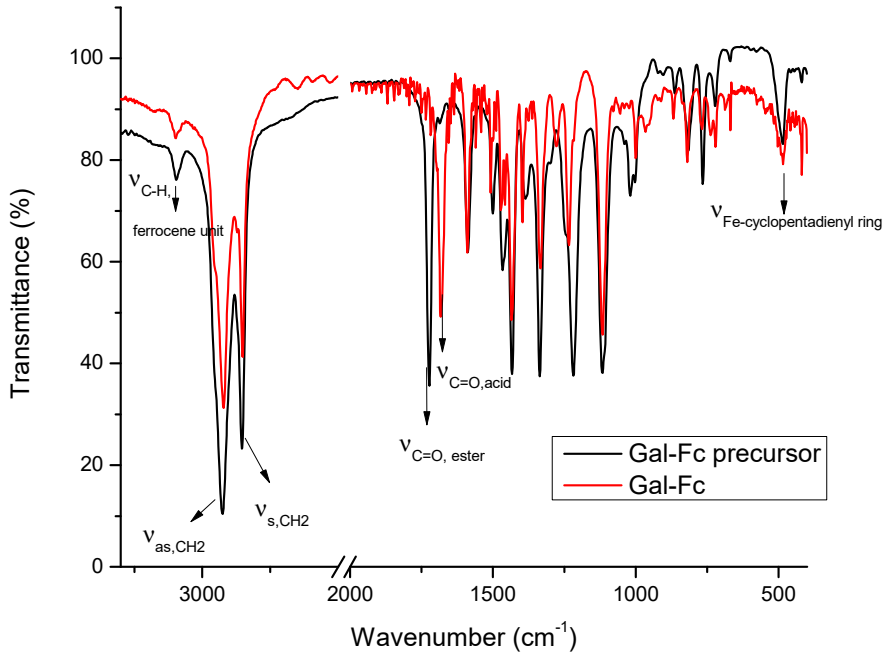

Figure 2. FT-IR spectrum of Gal-Fc plotted vs. Gal-Fc_precursor.

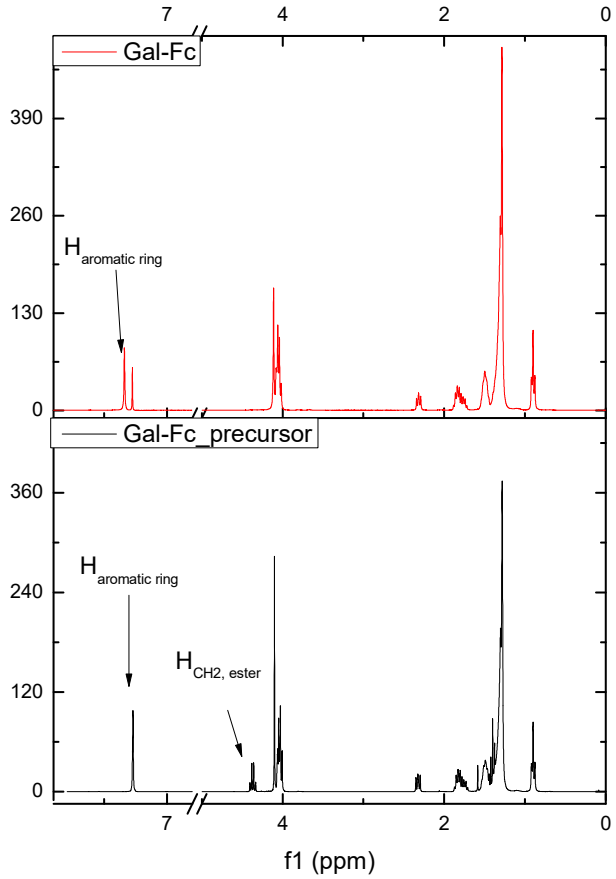

Figure 3. ^{1}H-NMR spectra of Gal-Fc_precursor and Gal-Fc.

The spectra of the compounds Gal-Fc_precursor and Gal-Fc (Figure 2) presented the expected characteristic absorption bands for asymmetric (2925 cm^{-1}) and symmetric (2855 cm^{-1}) stretching vibration for the carbon–hydrogen bond belonging to the methylene groups present in the molecule [44]. Moreover, the presence of the ferrocene unit was confirmed by the presence of the characteristic absorption band of the stretching vibration of the carbon–hydrogen bond from the cyclopentadienyl ring, around 3091 cm^{-1}, and at about 485 cm^{-1}, that characteristic for the stretching vibration band between Fe(II) and the cyclopentadienyl ring [45]. By comparing the spectra of Gal-Fc with that of its precursor, Gal-Fc_precursor, the successful conversion to the corresponding carboxylic acid was confirmed by e-shifting the characteristic absorption band of the carbonyl group from 1719 cm^{-1} in Gal-Fc_precursor to 1678 cm^{-1} in Gal-Fc.

The ^{1}H-NMR (Figure 3) further confirmed the above results due to the chemical shifts of the aromatic proton from the gallate unit from 7.27 ppm in Gal-Fc_precursor (overlapped with the signals of $CDCl_3$) to 7.34 ppm in case of Gal-Fc. Further confirmation on the formation of the carboxylic acid was evidenced from the disappearance of the proton corresponding to the methylene group of the ester.

Finally, the purity of the Gal-Fc compound used for electrochemical studies was checked through an elemental analysis (Experimental section in Supplementary Material).

3.1. Testing of Voltammetric Methods

3.1.1. Cyclic Voltammetry (CV)

Taking into account the results presented already for the Gal-Fc modified CNT paste electrode via drop casting under the potential range from −1.50 to +1.00 V/SCE [26], the CV shapes recorded for the Gal-Fc-CNT paste electrode at various pH values of 3, 5, and 12 under an enlarged potential range to the cathodic branch (presented in Figure 4) manifest a ferrocene/ferrocenium redox couple, further ferrocenium oxidation, and an Fe/Fe(II)

redox couple, where oxidation peaks occurred at more negative potential values of about −0.66 V vs. SCE, as well as the corresponding reduction peak at about −1.00 V vs. SCE. The CNT oxidation and reduction processes are not visible, probably due to the fact that they are overlapped by the redox couples of the Fe species.

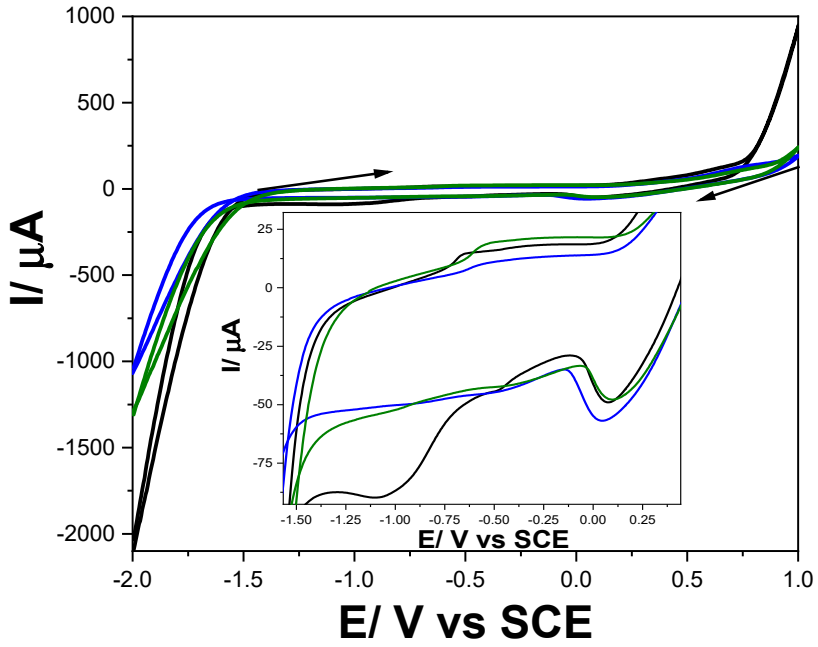

Figure 4. Cyclic voltammograms recorded at a scan rate of 0.05 $V \cdot s^{-1}$ with Gal-Fc-CNT paste electrode in the 0.1 M NaOH supporting electrolyte (pH = 12 (black line)), 0.1 M Na_2SO_4 adjusted at pH = 3 (blue line), and 0.1 M Na_2SO_4 adjusted at pH = 5 (green line), within the potential range of −2.0 to +1.0 V/SCE.

As we expected, from a thermodynamic point of view, the alkaline medium favored the oxygen and hydrogen evolution and the peaks corresponding to the redox couples are better evidenced, especially the Fe (II) reduction at the potential value of −1.00 V/SCE.

The electrochemical behavior of the Gal-Fc-CNT paste electrode was tested at each pH value in the presence of 1 $mg \cdot L^{-1}$ of DOX, CPB, and CPP from the cytostatics class (examples are presented in Supplementary material—Figure S1a–c). The utile signals reached at each pH value are gathered in Table 1.

Table 1. The utile signals found for DOX, CPB, and CPP at each pH value.

pH	DOX		CPB		CPP	
	E/V vs. SCE	ΔI/ µA/mg·L^{-1}	E/V vs. SCE	ΔI/µA/mg·L^{-1}	E/V vs. SCE	ΔI/µA/mg·L^{-1}
3	−0.46	0.51	−0.46	-	−0.46	-
5	−0.46	4.05	−0.46	3.25	−0.50	2.76
12	−0.60	5.41	−0.60	4.13	−0.60	3.04

It can be noticed that at pH values of 12 and 5, all cytostatics gave anodic utile signals, which were better at a pH of 12, while for pH 3, only DOX exhibited an anodic utile signal. Based on these findings, two approaches were considered to develop the method for their simultaneous determination and for the selective determination of DOX.

The electrochemical behavior of the Gal-Fc-CNT paste electrode in the presence of 1 to 5 $mg \cdot L^{-1}$ of CPP, CPB, and DOX at a pH of 12 are presented in Figure 5.

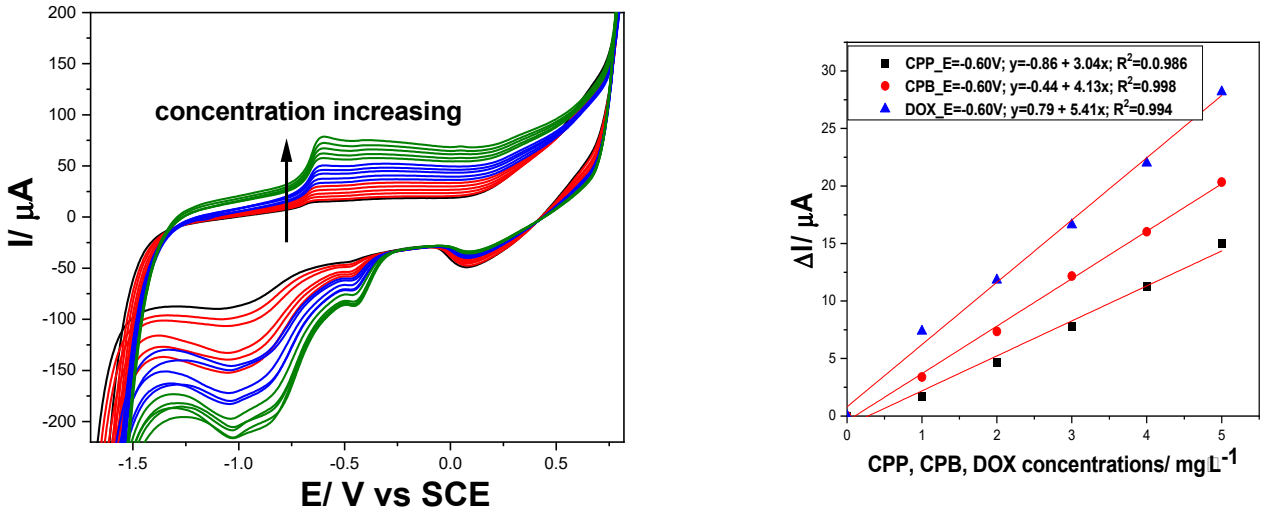

(**a**) (**b**)

Figure 5. (**a**) CVs recorded with Gal-Fc-CNT paste electrode in 0.1 M NaOH supporting electrolyte (black line) within the potential range from −2.00 to +1.00 V/SCE at the scan rate of 0.05 $V \cdot s^{-1}$ in the presence of 1–5 $mg \cdot L^{-1}$ of CPP (red line); 1–5 $mg \cdot L^{-1}$ of CPB (blue line); 1–5 $mg \cdot L^{-1}$ of DOX (green line). (**b**) Linear dependence of the anodic peak current recorded at −0.60 V vs. CPP, CPB, and DOX concentrations.

Similar behavior was observed for each cytostatic, which oxidized starting with the potential value corresponding to Fe (II) oxidation at about −0.60 V/SCE, with more steps also involving the ferrocene/ferrocenium redox couple at the potential value of about +0.25 V vs. SCE. Also, the cathodic responses involving Fe (II) reduction at about −1.00 V/SCE are noticed to have not increased linearly with the cytostatic concentration, probably due to the complexity of the reduction reactions of each compound and their byproducts.

The electrochemical behavior of the Gal-Fc-CNT electrode in the potential window from −1.50 to +1.00 V/SCE in the presence of 1 to 3 $mg \cdot L^{-1}$ of CPP, CPB, and DOX at a pH of 3 are presented in Figure 6.

It is obvious that at a pH of 3, only DOX is oxidized at −0.30 V/SCE, generating an analytical signal of 0.30 $\mu A/mg \cdot L^{-1}$, which is lower in comparison with that obtained at a pH of 12. No anodic peak current increased in the presence of CPB and CPP because no oxidation occurred, which can be exploited for the further development of the selective determination of DOX in the presence of CPP and CPB. Also, the cathodic signal related to the anodic one can be seen only in the presence of DOX.

For better evidence of the effect of pH on DOX oxidation, the influence of the scan rate on the CV shapes in the presence of 2 $mg \cdot L^{-1}$ of DOX at pHs of 3 and 12 was studied. The results involving the utile current dependence versus the square root of the scan rate and oxidation/reduction potential dependences versus the logarithm of the scan rate are presented in Figures 7a–c and 8a–c at increasing scan rates ranging from 10 to 200 $mV \cdot s^{-1}$. The differences between the series of CVs are related to the lower potential value for O_2 and H_2 evolution, similar to the results obtained in the absence of an analyte, as presented in Figure 4. Also, the Fe species and ferrocene-based redox couples are more evidenced in the alkaline medium, probably because some oxides are formed, which exhibits better electrocatalytic activity.

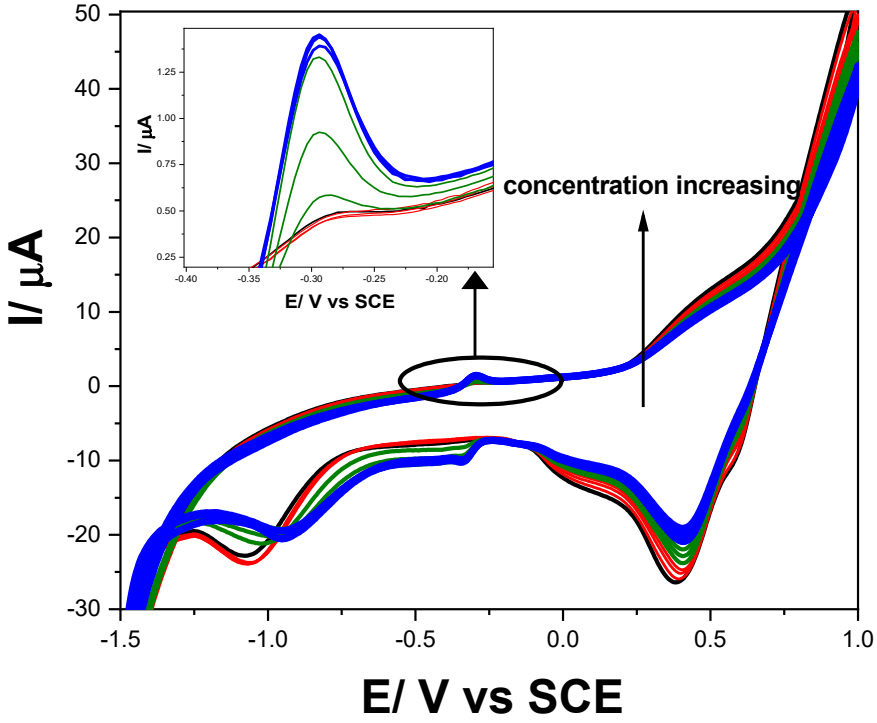

Figure 6. CVs recorded with Gal-Fc-CNT paste electrode in 0.1 M Na_2SO_4 adjusted at pH = 3 (black line) within the potential range from −1.50 to +1.00 V/SCE at the scan rate of 0.05 $V \cdot s^{-1}$ in the presence of 1–3 $mg \cdot L^{-1}$ of CPP (red line); 1–3 $mg \cdot L^{-1}$ of DOX (green line); 1–3 $mg \cdot L^{-1}$ of CPB (blue line). Inset: detail of CVs.

The linear dependence of the utile anodic and cathodic currents for 2 $mg \cdot L^{-1}$ of DOX, determined by eliminating the supporting electrolyte currents vs. the square root of the scan rate, are expressed by Equations (1) at pH = 12 and (2) at pH = 3:

$$\text{pH = 12: } \Delta Ia = 440.67\ v^{1/2} - 46.20\ (E = -0.60\ V);\ \Delta Ia = 603.03\ v^{1/2} - 59.65\ (E = +0.34\ V);\ \Delta Ic = -642.40\ v^{1/2} + 12.88\ (E = -1.00\ V) \quad (1)$$

$$\text{pH = 3: } \Delta Ia = 140.67\ v^{1/2} - 16.31\ (E = -0.60\ V);\ \Delta Ia = 233.36\ v^{1/2} - 18.75\ (E = +0.34\ V);\ \Delta Ic = -328.36\ v^{1/2} + 26.44\ (E = -1.00\ V) \quad (2)$$

It should be mentioned that at a pH of 3, the utile signal appeared only at scan rates higher than 40 $mV \cdot s^{-1}$, suggesting a faster kinetics of the DOX oxidation process in comparison with pH = 12. This behavior should be explained by the instability of DOX at pH = 3, generating doxorubicinone and daunosamine [46], which are further oxidized. This aspect can be responsible for the difference between the process rates at pH = 12 vs. pH = 3. Also, no zero reverse interception was present, suggesting a very complex mechanism for all oxidation and reduction processes responsible for DOX determination, and moreover, no ideal reversible character is suggested by the results of the E-log vs. dependence.

Considering that the literature data related to DOX electrochemical determination mechanisms [21,23,32] corroborated the above-presented results, two-electron based DOX electrooxidation and electroreduction involving Fe species and ferrocene redox couples are proposed for both pHs of 12 and 3, with very fast kinetics at pH 3. Also, the two-electron oxidation and reduction processes are proposed for CPP and its oxidized form in accordance with the literature data [42] and for CPB oxidation and reduction, also as reported in the literature [47–49]. The lack of anodic and cathodic peak current intensification with increasing CPP and CPB concentrations at pH 3 should be explained by much lower kinetics or the lack of their oxidation and reduction processes in comparison with DOX ones.

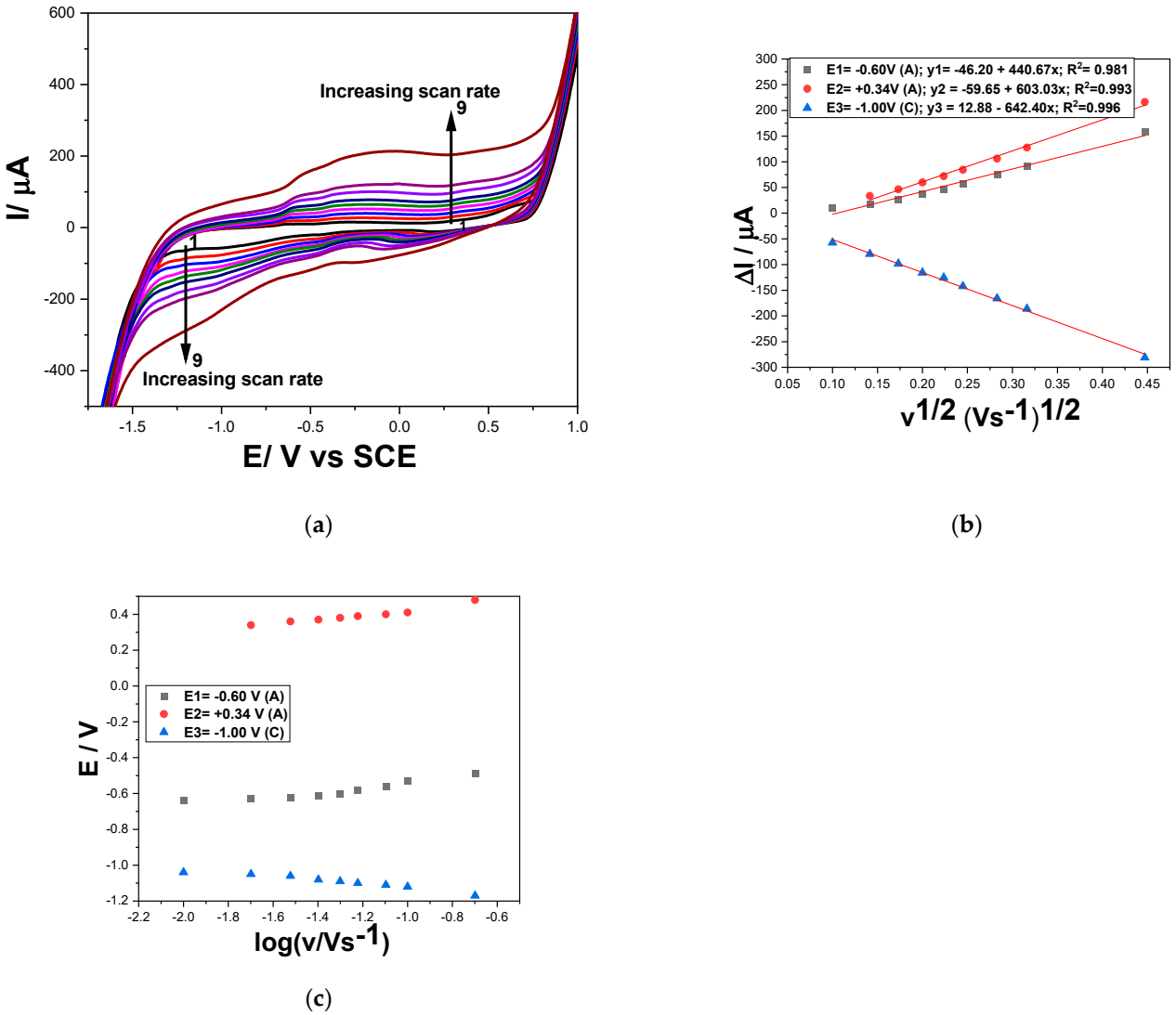

(**a**) (**b**)

(**c**)

Figure 7. (**a**) CVs recorded at various scan rates ranging from 10 mV·s^{-1} to 200 mV·s^{-1} (curves: 1–9) with the Gal-Fc-CNT paste electrode in 0.1 M NaOH supporting electrolyte (pH = 12), and in the presence of 2 mg·L^{-1} DOX concentration. (**b**) Dependence of anodic and cathodic peak current vs. square root of the scan rate. (**c**) Dependence of anodic and cathodic peak potentials vs. logarithm of the scan rate.

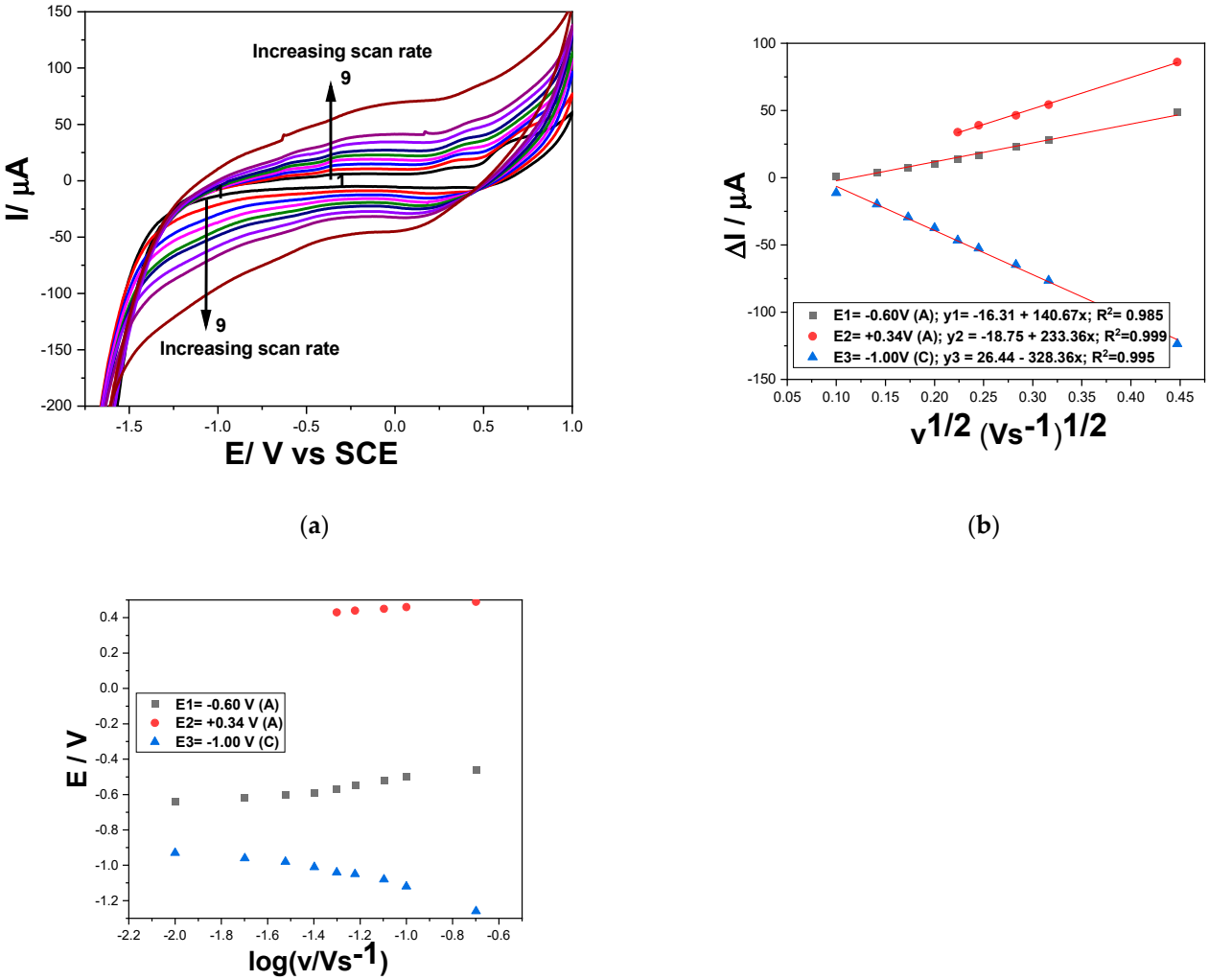

Figure 8. (**a**) CVs recorded at various scan rates ranging from 10 mV·s^{-1} to 200 mV·s^{-1} (curves: 1–9) with the Gal-Fc-CNT paste electrode in 0.1 M Na_2SO_4 adjusted at pH = 3, and in the presence of 2 mg·L^{-1} DOX concentration. (**b**) Dependence of anodic and cathodic peak current vs. square root of the scan rate. (**c**) Dependence of anodic and cathodic peak potentials vs. logarithm of the scan rate.

3.1.2. Simultaneous Determination of Cytostatics/Selective Determination of DOX Using Differential-Pulsed and Square-Wave Voltammetry Techniques

In view of the improvement of the electroanalytical performance for both the simultaneous determination of DOX, CPB, and CPP at pH 12 and for the selective determination of DOX at pH 3, it was employed that DPV is characterized by significantly diminishing the current background as well as more evidenced oxidation and reduction peaks. The operating parameters are optimized related to the electrode's composition considering the sensitivity and the electrode stability. Thus, the best results at pH 12 were achieved for a modulation amplitude of 100 mV, a step potential of 25 mV, and a scan rate of 0.05 V·s^{-1} (Figure 9a), and at pH 3, the modulation amplitude was 200 mV, the step potential was 25 mV, and the similar scan rate was 0.05 V·s^{-1} (Figure 9b).

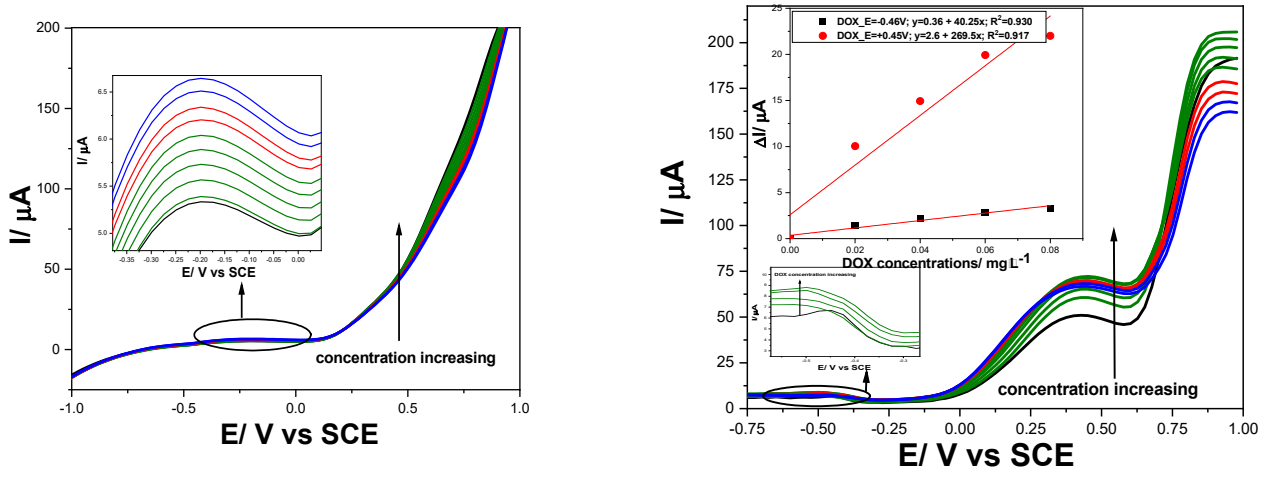

(**a**) (**b**)

Figure 9. (**a**) Differential-pulse voltammograms (detail) recorded with Gal-Fc-CNT paste electrode in 0.1 M NaOH supporting electrolyte (black curve), pH = 12, in the presence of different DOX concentrations (2–10 $\mu g \cdot L^{-1}$ DOX (green curves)), and in the presence of 100 and 200 $\mu g \cdot L^{-1}$ CPP (red curves) and 100 and 200 $\mu g \cdot L^{-1}$ CPB concentrations (blue curves); at 25 mV step potential, 100 mV modulation amplitude, 50 $mV \cdot s^{-1}$ potential scan rate, and potential range of −1.50 to +1.00 V vs. SCE. (**b**) Differential-pulse voltammograms (detail) recorded with Gal-Fc-CNT paste electrode in 0.1 M Na_2SO_4 adjusted at pH = 3 (black curve), in the presence of different DOX concentrations (20–100 $\mu g \cdot L^{-1}$ DOX (green curves)), and in the presence of 100 and 200 CPP $\mu g \cdot L^{-1}$ (red curves) and 100–200 $\mu g \cdot L^{-1}$ CPB concentrations (blue curves), at 25 mV step potential, 200 mV modulation amplitude, 50 $mV \cdot s^{-1}$ potential scan rate, and potential range of −1.50 to +1.00 V vs. SCE. Inset: calibration plots of the currents recorded at E = −0.46 V and +0.45 V/SCE vs. DOX concentrations.

At pH 12, for the simultaneous determination of DOX, CPB, and CPP, at the detection potential of −0.20 V/SCE, better sensitivities were achieved through DPV in comparison with CV, thus leading to 73.71 $\mu A/mg \cdot L^{-1}$ compared with 5.41 $\mu A/mg \cdot L^{-1}$ for DOX, 5.00 $\mu A/mg \cdot L^{-1}$ compared with 4.13 $\mu A/mg \cdot L^{-1}$ for CPB, and 6.55 $\mu A/mg \cdot L^{-1}$ compared with 3.04 $\mu A/mg \cdot L^{-1}$ for CPP.

At pH 3, for the selective determination of DOX at the detection potential value of −0.46 V/SCE, the sensitivity for DOX determination via DPV was 40.25 $\mu A/mg \cdot L^{-1}$ (compared with 0.30 $\mu A/mg \cdot L^{-1}$ via CV) and 269.5 $\mu A/mg \cdot L^{-1}$ at the potential value of +0.45 V/SCE, at which no signal was achieved with CV. The increasing current at the potential value of +0.45 V/SCE informed on the ferrocene redox couple's involvement in DOX oxidation under acidic media.

Also, considering the peculiarities of SWV as the fastest voltammetry technique, various operating conditions were tested for optimization for both cytostatic simultaneous determination and DOX selective determination. For the simultaneous determination of cytostatics at a pH of 12, a modulation amplitude of 100 mV, a step potential of 4 mV, a frequency of 25 Hz, and a 100 $mV \cdot s^{-1}$ potential scan rate (Figure 10a) were used. Similar conditions, except for the frequency of 50 Hz, which assured a double potential scan rate of 200 $mV \cdot s^{-1}$, were found to be optimum for the selective determination of DOX at pH 3 (Figure 10b).

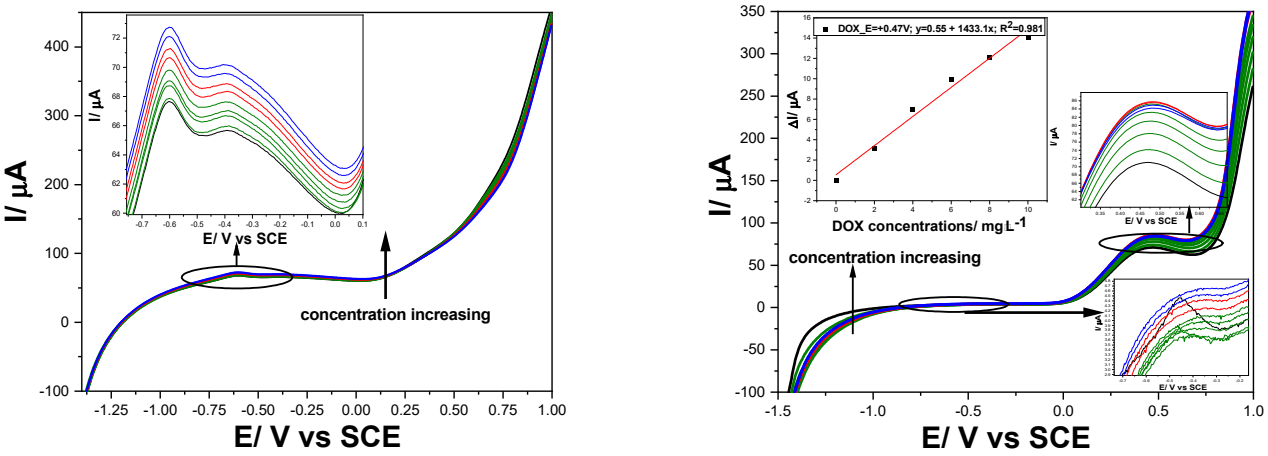

(**a**) (**b**)

Figure 10. (**a**) Square-wave voltammograms (detail) recorded with Gal-Fc-CNT paste electrode in 0.1 M NaOH supporting electrolyte (black curve), pH = 12, in the presence of different DOX concentrations (4–10 $\mu g \cdot L^{-1}$ DOX (green curves)), and in the presence of 100 and 200 $\mu g \cdot L^{-1}$ CPP (red curves) and 100 and 200 $\mu g \cdot L^{-1}$ CPB (blue curves); 4 mV step potential, 100 mV modulation amplitude, frequency = 25 Hz, 100 $mV \cdot s^{-1}$ potential scan rate, potential range: −1.50 to +1.00 V/SCE. (**b**) Square-wave voltammograms (detail) recorded with Gal-Fc-CNT paste electrode in 0.1 M Na_2SO_4 adjusted at pH = 3 (black curve), in the presence of different DOX concentrations (2–10 $\mu g \cdot L^{-1}$ DOX (green curves)), and in the presence of 100 and 200 $\mu g \cdot L^{-1}$ CPP (red curves) and 100 and 200 $\mu g \cdot L^{-1}$ CPB concentrations (blue curves); 4 mV step potential, 100 mV modulation amplitude, frequency = 50 Hz, 200 $mV \cdot s^{-1}$ potential scan rate, potential range: −1.50 to +1.00 V vs. SCE. Inset: calibration plots of the currents recorded at E = +0.47 V/SCE vs. DOX concentrations.

These optimum conditions generated better sensitivities than those obtained using DPV at a response time equal to half, or even a quarter, of that of DPV. The comparative sensitivities of both voltammetric techniques are compared in Table 2.

Table 2. Comparative utile signals achieved for simultaneous determination of DOX, CPB, and CPP at pH of 12.

Technique	DOX		CPB		CPP	
	E/V vs. SCE	ΔI/ µA/mg·L^{-1}	E/V vs. SCE	ΔI/µA/mg·L^{-1}	E/V vs. SCE	ΔI/µA/mg·L^{-1}
DPV	−0.20	73.71	−0.20	5.00	−0.20	6.55
SWV	−0.60	311.9	−0.60	22.90	−0.60	30.25

It can be concluded that SWV exhibits great potential for either the fast simultaneous determination of DOX, CPB, and CPP or the selective determination of DOX, with better sensitivities in comparison with CV and DPV.

The limit of detection was also achieved using SWV for both simultaneous cytostatic determination and the selective determination of DOX (see Supplementary Material—Table S1). Thus, the lowest limits of detection of 0.71 $\mu g \cdot L^{-1}$ at pH = 12 and 0.75 $\mu g \cdot L^{-1}$ at pH = 3 were achieved for DOX, and at pH = 12, the lowest limits of detection of 13 $\mu g \cdot L^{-1}$ for CPB and 9 $\mu g \cdot L^{-1}$ for CPP were reached for their simultaneous determination. It is obvious that a cumulative voltammetric signal is achieved for cytostatic determination at pH 12 and a detection potential of −0.60 V/SCE as a sum of their concentrations that can be proposed as *a cytostatic index*. Also, the selective quantitative determination of DOX at pH 3 and a detection potential of +0.5 V/SCE offers the possibility to assess its contribution to the *cytostatic index*.

Besides the possibility to assess the *cytostatic index* and selective determination of DOX, the limits of detection are similar and quite better in comparison with the reported data related to only the individual detection of these cytostatics (Table 3).

Table 3. The performance of Gal-Fc-CNT paste electrode in comparison with reported ones.

Electrode	Analyte	LOD	Method	Reference
CDs-5.0/MgO/SPCE [a]	DOX	90 nM	CV	[31]
Pt/MWCNTs [b]	DOX	3.7 nM	CV	[32]
graphite-based disposable SPE [c]	DOX/Simvastatin *	180 nM 2.78 µM	CA LSV	[33]
CuNPs-CB-Nafion/GCE [d]	DOX/ Methotrexate *	24 nM	SWV	[34]
MOF-235/GO nanocomposite modified CPE [e]	DOX	5 nM	CV	[35]
SNPs@MOF/BNSs-Fc/GCE [f]	DOX	2 nM	SWV	[36]
p-AgSAE [g]	DOX	0.84 µM	DPCSV	[38]
ZnO/MWCNTs/CPE [h]	CPB	30 nM	DPV	[10]
AuNPs/SGNF-modified GCE [i]	CPB	17 nM	DPV	[39]
MWCNT-PUFIX/HF-PGE [j]	CPB/Erlotinib *	0.110 µM	DPV	[40]
GCE [k]	CPP	1.1 µM	CV	[41]
Current work	DOX/CPB/CPP *	1.13/30/32 nM	SWV	-

* Simultaneous; [a] CDs-5.0/MgO/SPCE—carbon dots/magnesium oxide-modified screen-printed carbon electrodes; [b] Pt/MWCNTs—multi-walled carbon nanotube-modified platinum electrode; [c] graphite-based disposable SPE—graphite-based disposable screen-printed electrodes; [d] CuNPs-CB-Nafion/GCE—carbon black–copper nanoparticles–Nafion-modified glassy carbon electrode; [e] MOF-235/GO nanocomposite modified CPE—carbon paste electrode modified by a nanocomposite containing graphene oxide and metal organic framework-235; [f] SNPs@MOF/BNSs-Fc/GCE—sulfur nanoparticle-encapsulated cobalt metal–organic framework/boron nanosheets–ferrocene complex/glassy carbon electrode; [g] p-AgSAE—silver solid amalgam electrode; [h] ZnO/MWCNTs/CPE—zinc oxide nanoparticles/multi-walled carbon nanotube-modified carbon paste electrode; [i] AuNPs/SGNF-modified GCE—glassy carbon electrode modified by gold nanoparticles and stacked graphene nanofibers; [j] MWCNT-PUFIX/HF-PGE—pencil graphite electrode modified with multi-walled carbon nanotubes–polyurethane nanocomposite/polypropylene hollow fiber; [k] GCE—glassy carbon electrode.

The accuracy and precision of the SWV method using the Gal-Fc-CNT paste electrode were checked through recovery experiments. The different concentrations of DOX, CPB, and CPP were spiked to the tap water sample and three replicate measurements were performed for each sample at pH = 12 and at pH = 3. The standard addition method was applied for both the simultaneous determination of DOX, CPB, and CPP at pH = 12 and the selective determination of DOX at pH = 3 in the real water sample. No cytostatics were found in the real tap water from Timisoara city, Romania. The recovery degree values were close to 100% (102.50–104.25%, 98.75–99.80%, and 97.40–98.50% for DOX, CPB, and CPP, respectively) at pH = 12, and 101.20–104.80% at pH = 3 (the results are presented in Supplementary material—Table S2) indicates the accuracy of the SWV-based method when using the CNT-Fc paste electrode, which shows its suitability for practical application in screening real water samples, considering the cytostatics index and DOX quantification.

4. Conclusions

A gallic acid derivative functionalized with long alkyl chains containing a ferrocene unit inserted into the hydrophilic part of the molecule was chosen as a modifier of a CNT paste electrode due to the presence of active electrochemical centers like ferrocene and carboxylic functional groups in a single molecule.

A ferrocene-containing gallic acid-derivative modified carbon-nanotube paste electrode (Gal-Fc-CNT), obtained through simple mechanical mixing, exhibited redox-based

advanced electrochemical properties that are useful for the development of the simultaneous determination of doxorubicin, capecitabine, and cyclophosphamide as *cytostatic indices*.

The Fe species redox couples, together with the ferrocene/ferrocenium redox couple, exhibited electrocatalytic activity towards cytostatic oxidation and/or their byproduct reduction related to the pH values and the potential range. The best electrocatalytic activity was manifested by the Fe/Fe(II) redox couple under a pH of 12 in the potential window of −2.00 and +1.00 V/SCE towards all tested cytostatic oxidation via two-electron transfer, controlled through a diffusion step that assured their simultaneous cumulative assessment by the cytostatic index at the unusual oxidation potential value of −0.60 V/SCE. The best electroanalytical performance was achieved by using the square-wave voltammetry technique, operated at a modulation amplitude of 100 mV, a step potential of 4 mV, a frequency of 25 Hz, and a 100 $mV \cdot s^{-1}$ potential scan rate that allowed us to reach the limits of detection of 71 $ng \cdot L^{-1}$ for doxorubicin, 13 $\mu g \cdot L^{-1}$ for capecitabine, and 9 $\mu g \cdot L^{-1}$ for cyclophosphamide.

At pH 3 only doxorubicin gave an increasing signal based on the faster kinetics of its oxidation in comparison with the other cytostatics, which allowed its faster selective determination with similar electroanalytical performance. Thus, the limit of detection of 75 $ng \cdot L^{-1}$ was achieved for doxorubicin using the square-wave voltammetry technique, operated at a modulation amplitude of 100 mV, a step potential of 4 mV, a frequency of 50 Hz, and a 200 $mV \cdot s^{-1}$ potential scan rate.

The Gal-Fc-CNT paste electrode showed good reproducibility, stability, and the ability to measure the cumulative effect of DOX, CPB, and CPP simultaneously as a *cytostatic index*, as well as DOX concentrations, selectively in real tap water samples (Timisoara city, Romania), indicating its great potential for practical applications in the analysis of different water samples.

Supplementary Materials: The following supporting information can be downloaded at https://www.mdpi.com/article/10.3390/chemosensors12010015/s1: Scheme S1: Synthetic pathway for the synthesis of Gal-Fc; Figure S1: CVs recorded with CNT-Gal-Fc electrode in 0.1 M NaOH supporting electrolyte within the potential range from −2.00 to +1.00 V/SCE at the scan rate of 0.05 $V \cdot s^{-1}$ in the presence of (a) 1–5 $mg \cdot L^{-1}$ CPP (red line); (b) 1–5 $mg \cdot L^{-1}$ CPB (blue line); (c) 1–5 $mg \cdot L^{-1}$ DOX (green line). Table S1: The electroanalytical performance obtained with CNT-Gal-Fc paste electrode in 0.1 M NaOH supporting electrolyte; Table S2. Recovery degrees achieved with Gal-Fc-CNT paste electrode using SWV for tap water spiked with known cytostatics concentrations.

Author Contributions: Conceptualization, F.M.; methodology, F.M., A.V. and S.M.; investigation, S.M., A.A., A.B. and A.V.; formal analysis, A.V. and A.B.; resources, A.A.; writing—original draft preparation, F.M., S.M., A.B. and A.A.; writing—review and editing, F.M. and E.I.S. All authors have read and agreed to the published version of the manuscript.

Funding: This work was supported by a grant from the Ministry of Research, Innovation and Digitization, CNCS/CCCDI—UEFISCDI, project number PN-III-P1-1.1-PD-2021-0427, within PNCDI III, and partially by a grant from the Romanian Ministry of Education and Research, "Program intern de stimulare si recompensare a activitatii didactice", contract number 10161/11 June.

Institutional Review Board Statement: Not applicable.

Informed Consent Statement: Not applicable.

Data Availability Statement: No new data were created or analyzed in this study.

Conflicts of Interest: The authors declare no conflicts of interest.

References

1. Patel, M.; Kumar, R.; Kishor, K.; Mlsna, T.; Pittman, C.U.; Mohan, D. Pharmaceuticals of Emerging Concern in Aquatic Systems: Chemistry, Occurrence, Effects, and Removal Methods. *Chem. Rev.* **2019**, *119*, 3510–3673. [CrossRef] [PubMed]
2. Jureczko, M.; Kalka, J. Cytostatic pharmaceuticals as water contaminants. *Eur. J. Pharmacol.* **2020**, *866*, 172816. [CrossRef] [PubMed]

3. Waleng, N.J.; Nomngongo, P.N. Occurrence of Pharmaceuticals in the Environmental Waters: African and Asian Perspectives. *Environ. Chem. Ecotoxicol.* **2022**, *4*, 50–66. [CrossRef]
4. Hughes, S.R.; Kay, P.; Brown, L.E. Global Synthesis and Critical Evaluation of Pharmaceutical Data Sets Collected from River Systems. *Environ. Sci. Technol.* **2013**, *47*, 661–677. [CrossRef]
5. Ferlay, J.; Colombet, M.; Soerjomataram, I.; Parkin, D.M.; Pineros, M.; Znaor, A.; Bray, F. Cancer Statistics for the Year 2020: An Overview. *Int. J. Cancer* **2021**, *149*, 778–789. [CrossRef] [PubMed]
6. Zhang, J.; Chang, V.W.C.; Giannis, A.; Wang, J.Y. Removal of Cytostatic Drugs from Aquatic Environment: A Review. *Sci. Total Environ.* **2013**, *445–446*, 281–298. [CrossRef]
7. Gouveia, T.I.A.; Alves, A.; Santos, M.S.F. New Insights on Cytostatic Drug Risk Assessment in Aquatic Environments Based on Measured Concentrations in Surface Waters. *Environ. Int.* **2019**, *133*, 105236. [CrossRef] [PubMed]
8. Feier, B.; Florea, A.; Cristea, C.; Sandulescu, R. Electrochemical Detection and Removal of Pharmaceuticals in Waste Waters. *Curr. Opin. Electrochem.* **2018**, *11*, 1–11. [CrossRef]
9. Huang, B.; Xiao, L.; Dong, H.; Zhang, X.; Gan, W.; Mahboob, S.; Al-Ghanim, K.A.; Yuan, Q.; Li, Y. Electrochemical Sensing Platform Based on Molecularly Imprinted Polymer Decorated N,S Co-doped Activated Graphene for Ultrasensitive and Selective Determination of Cyclophosphamide. *Talanta* **2017**, *164*, 601–607. [CrossRef]
10. Madrakian, T.; Ghasemi, H.; Haghshenasa, E.; Afkhamia, A. Preparation of a ZnO Nanoparticles/Multiwalled Carbon Nanotubes/Carbon Paste Electrode as a Sensitive Tool for Capecitabine Determination in Real Samples. *RSC Adv.* **2016**, *6*, 33851–33856. [CrossRef]
11. Booker, V.; Halsall, C.; Llewellyn, N.; Johnson, A.; Williams, R. Prioritising Anticancer Drugs for Environmental Monitoring and Risk Assessment Purposes. *Sci. Total Environ.* **2014**, *473–474*, 159–170. [CrossRef] [PubMed]
12. Gomez-Canela, C.; Cortes-Francisco, N.; Ventura, F.; Caixach, J.; Lacorte, S. Liquid Chromatography Coupled to Tandem Mass Spectrometry and High-Resolution Mass Spectrometry as Analytical Tools to Characterize Multi-class Cytostatic Compounds. *J. Chromatogr. A* **2013**, *1276*, 78–94. [CrossRef] [PubMed]
13. Santana-Viera, S.; Hernandez-Arencibia, P.; Sosa-Ferrera, Z.; Santana-Rodriguez, J.J. Simultaneous and Systematic Analysis of Cytostatic Drugs in Wastewater Samples by Ultra-High Performance Liquid Chromatography Tandem Mass Spectrometry. *J. Chromatogr. B* **2019**, *1110–1111*, 124–132. [CrossRef]
14. Omanovic, D.; Garnier, C.; Gibbon–Walsh, K.; Pizeta, I. Electroanalysis in Environmental Monitoring: Tracking Trace Metals—A Mini Review. *Electrochem. Commun.* **2015**, *61*, 78–83. [CrossRef]
15. Uslu, B.; Ozkan, S. Electroanalytical Application of Carbon-Based Electrodes to the Pharmaceuticals. *Anal. Lett.* **2007**, *40*, 817–853. [CrossRef]
16. Boumya, W.; Taoufik, N.; Achak, M.; Barka, N. Chemically Modified Carbon-Based Electrodes for the Determination of Paracetamol in Drugs and Biological Samples. *J. Pharm. Anal.* **2021**, *11*, 138–154. [CrossRef]
17. Huseinov, A.; Nawarathne, C.P.; Alvarez, N.T. Chemically Bonded Carbon Nanotube Film to a Nanostructured Gold Electrode for Electrochemical Sensing of Hydrogen Peroxide. *ACS Appl. Nano Mater.* **2023**, *6*, 20082–20088. [CrossRef]
18. Nardi, N.; Baumgarten, L.G.; Dreyer, J.P.; Santana, E.R.; Winiarski, J.P.; Cruz Vieira, I. Nanocomposite Based on Green Synthesis of Gold Nanoparticles Decorated with Functionalized Multi-Walled Carbon Nanotubes for the Electrochemical Determination of Hydroxychloroquine. *J. Pharm. Biomed. Anal.* **2023**, *236*, 115681. [CrossRef]
19. Motoc, S.; Manea, F.; Orha, C.; Pop, A. Enhanced Electrochemical Response of Diclofenac at a Fullerene–Carbon Nanofiber Paste Electrode. *Sensors* **2019**, *19*, 1332. [CrossRef]
20. Ilies, S.; Schinteie, B.; Pop, A.; Negrea, S.; Cretu, C.; Szerb, E.I.; Manea, F. Graphene Quantum Dots and Cu(I) Liquid Crystal for Advanced Electrochemical Detection of Doxorubicine in Aqueous Solutions. *Nanomaterials* **2021**, *11*, 2788. [CrossRef]
21. Motoc, S.; Manea, F.; Baciu, A.; Orha, C.; Pop, A. Electrochemical Method for Ease Determination of sodium Diclofenac Trace Levels in Water Using Graphene—Multi-Walled Carbon Nanotubes Paste Electrode. *Int. J. Environ. Res. Public Health* **2022**, *19*, 29. [CrossRef]
22. Motoc, S.; Manea, F.; Baciu, A.; Vasilie, S.; Pop, A. Highly Sensitive and Simultaneous Electrochemical Determinations of Non-Steroidal Anti-Inflammatory Drugs in Water Using Nanostructured Carbon-Based Paste Electrodes. *Sci. Total Environ.* **2022**, *846*, 1574128. [CrossRef]
23. Saleh Ahammad, A.J.; Lee, J.J.; Rahman, M.A. Electrochemical Sensors Based on Carbon Nanotubes. *Sensors* **2009**, *9*, 2289–2319. [CrossRef]
24. Beitollahi, H.; Khalilzadeh, M.A.; Tajik, S.; Safaei, M.; Zhang, K.; Jang, H.W.; Shokouhimehr, M. Recent Advances in Applications of Voltammetric Sensors Modified with Ferrocene and Its Derivatives. *ACS Omega* **2020**, *5*, 2049–2059. [CrossRef]
25. Rauf, U.; Shabir, G.; Bukhari, S.; Albericio, F.; Saeed, A. Contemporary Developments in Ferrocene Chemistry: Physical, Chemical, Biological and Industrial Aspects. *Molecules* **2023**, *28*, 5765. [CrossRef] [PubMed]
26. Popa, E.; Andelescu, A.A.; Ilies, S.; Visan, A.; Cretu, C.; Scarpelli, F.; Crispini, A.; Manea, F.; Szerb, E.I. Hetero-Bimetallic Ferrocene-Containing Zinc(II)-Terpyridyl-Based Metallomesogen: Structural and Electrochemical Characterization. *Materials* **2023**, *16*, 1946. [CrossRef]
27. Kahkeshani, N.; Farzaei, F.; Fotouhi, M.; Alavi, S.S.; Bahramsoltani, R.; Naseri, R.; Momtaz, S.; Abbasabadi, Z.; Rahimi, R.; Farzaei, M.H.; et al. Pharmacological Effects of Gallic Acid in Health and Diseases: A Mechanistic Review. *Iran. J. Basic Med. Sci.* **2019**, *22*, 225–237. [CrossRef]

28. Badea, M.; di Modugno, F.; Floroian, L.; Tit, D.M.; Restani, P.; Bungau, S.; Iovan, C.; Badea, G.E.; Aleya, L. Electrochemical Strategies for Gallic Acid Detection: Potential for Application in Clinical, Food or Environmental Analyses. *Sci. Total Environ.* **2019**, *672*, 129–140. [CrossRef] [PubMed]
29. Wung, J.; Lu, J.; Larson, D.D.; Olsen, K. Voltammetric Sensor for Uranium Based on the Propyl Gallate Modified Carbon Paste Electrode. *Electroanalysis* **1995**, *7*, 247–250. [CrossRef]
30. Ganesh, H.V.S.; Noroozifar, M.; Kerman, K. Epigallocatechin Gallate-Modified Graphite Paste Electrode for Simultaneous Detection of Redox-Active Biomolecules. *Sensors* **2018**, *18*, 23. [CrossRef]
31. Singh, T.A.; Sharma, V.; Thakur, N.; Tejwan, N.; Sharma, A.; Das, J. Selective and Sensitive Electrochemical Detection of Doxorubicin via a Novel Magnesium Oxide/Carbon Dot Nanocomposite Based Sensor. *Inorg. Chem. Commun.* **2023**, *150*, 110527. [CrossRef]
32. Rus, I.; Tertis, M.; Barbalata, C.; Porfire, A.; Tomuta, I.; Sandulescu, R.; Cristea, C. An Electrochemical Strategy for the Simultaneous Detection of Doxorubicin and Simvastatin for Their Potential Use in the Treatment of Cancer. *Biosensors* **2021**, *11*, 15. [CrossRef]
33. Hajian, R.; Tayebi, Z.; Shams, N. Fabrication of an Electrochemical Sensor for Determination of Doxorubicin in Human Plasma and its Interaction with DNA. *J. Pharm. Anal.* **2017**, *7*, 27–33. [CrossRef]
34. Materon, E.M.; Wong, A.; Fatibello-Filho, O.; Faria, R.C. Development of a Simple Electrochemical Sensor for the Simultaneous Detection of Anticancer Drugs. *J. Electroanal. Chem.* **2018**, *827*, 64–72. [CrossRef]
35. Shamsadin-Azad, Z.; Taher, M.A.; Beitollahi, H. Metal Organic Framework-235/Graphene Oxide Nanocomposite Modified Electrode as an Electrochemical Sensor for the Voltammetric Determination of Doxorubicin in Presence of Dacarbazine. *Microchem. J.* **2024**, *196*, 109580. [CrossRef]
36. Yang, M.; Sun, Z.; Jin, H.; Gui, R. Sulfur Nanoparticle-Encapsulated MOF and Boron Nanosheet-Ferrocene Complex Modified Electrode Platform for Ratiometric Electrochemical Sensing of Adriamycin and Real-Time Monitoring of Drug Release. *Microchem. J.* **2022**, *177*, 107319. [CrossRef]
37. Jemelkova, Z.; Zima, J.; Barek, J. Voltammetric and amperometric determination of doxorubicin using carbon paste electrodes. *Collect. Czechoslov. Chem. Commun.* **2009**, *74*, 1503–1515. [CrossRef]
38. Skalova, S.; Langmaier, J.; Barek, J.; Vyskocil, V.; Navratil, T. Doxorubicin determination using two novel voltammetric approaches: A comparative study. *Electrochim. Acta* **2020**, *330*, 135180. [CrossRef]
39. Zhang, Q.; Shan, X.; Fu, Y.; Liu, P.; Li, X.; Liu, B.; Zhang, L.; Li, D. Electrochemical Determination of the Anticancer Drug Capecitabine Based on a Graphene-Gold Nanocomposite Modified Glassy Carbon Electrode. *Int. J. Electrochem. Sci.* **2017**, *12*, 10773–10782. [CrossRef]
40. Eshaghi, Z.; Moeipour, F. Carbon Nanotube/Polyurethane Modified Hollow Fiber-Pencil Graphite Electrode for In Situ Concentration and Electrochemical Quantification of Anticancer Drugs Capecitabine and Erlotinib. *Eng. Life Sci.* **2019**, *19*, 302–314. [CrossRef] [PubMed]
41. Sinha, P.; Doi, S.; Sharma, D.K. Electrochemical Behaviour and Adsorptive Stripping Voltammetric Determination of Cyclophosphamide. *Chem. Sci. Trans.* **2018**, *7*, 229–239. [CrossRef]
42. Baj-Rossi, C.; Micheli, G.D.; Carrara, S. Electrochemical Detection of Anti-Breast-Cancer Agents in Human Serum by Cytochrome P450-Coated Carbon Nanotubes. *Sensors* **2012**, *12*, 6520–6537. [CrossRef] [PubMed]
43. Kumar, K.; Vulugundam, G.; Kondaiah, P.; Bhattacharya, S. Co-liposomes of Redox-Active Alkyl-Ferrocene Modified Low MW Branched PEI and DOPE for Efficacious Gene Delivery in Serum. *J. Mater. Chem. B* **2015**, *3*, 2318–2330. [CrossRef]
44. Venkataraman, N.V.; Bhagyalakshmi, S.; Vasudevan, S.; Seshadri, R. Conformation and Orientation of Alkyl Chains in the Layered Organic–Inorganic Hybrids: $(C_nH_{2n+1}NH_3)_2PbI_4$ (n = 12,16,18). *Phys. Chem. Chem. Phys.* **2002**, *4*, 4533–4538. [CrossRef]
45. Radhakrishnan, S.; Paul, S. Conducting Polypyrrole Modified with Ferrocene for Applications in Carbon Monoxide Sensors. *Sens. Actuators B* **2007**, *125*, 60–65. [CrossRef]
46. Beijnen, J.H.; Wiese, G.; Underberg, W.J. Aspects of the chemical stability of doxorubicin and seven other anthracyclines in acidic solution. *Pharm. Weekbl.* **1985**, *7*, 109–116. [CrossRef]
47. Ljoncheva, M.; Kosjek, T.; Isidori, M.; Heath, E. 5-Fluorouracil and its prodrug capecitabine: Occurrence, fate and effect in environment. In *Fate and Effect of Anticancer Drugs in the Environment*; Isidori, M., Kosjek, T., Filipic, M., Eds.; Springer: Cham, Switzerland, 2020; pp. 331–375.
48. Dumitru, R.; Negrea, S.; Ianculescu, A.; Păcurariu, C.; Vasile, B.; Surdu, A.; Manea, F. Lanthanum Ferrite Ceramic Powders: Synthesis, Characterization and Electrochemical Detection Application. *Materials* **2020**, *13*, 2061. [CrossRef]
49. Rodrigues, H.; Lima, S.; da Silva, J.S.; de Oliveira Farias, E.A.; Sousa Teixeira, P.R.; Eiras, C.; Cunha Nunes, L.C. Electrochemical Sensors and Biosensors for the Analysis of Antineoplastic Drugs. *Biosens. Bioelectron.* **2018**, *108*, 27–37. [CrossRef]